CYBERNETICS AND PHYSICS, VOL. 6, NO. 3, 2017 , 114–120

MULTISTABILITY AND ITS CONTROL IN A SIMPLE CHAOTIC CIRCUIT WITH A PAIR OF LIGHT-EMITTING DIODES

Victor Kamdoum Tamba
Department of Telecommunication and Network Engineering
University of Dschang
Cameroon
vkamdoum@gmail.com

Hilaire Bertrand Fotsin
Department of Physics
University of Dschang
Cameroon
hbfotsin@yahoo.fr

Abstract

This paper investigates the multistability phenomenon and its control in a simple chaotic circuit with a pair of light emitting diodes proposed by Volos and collaborators (Nonlinear Dyn. 89:1047-1061, 2017). The bifurcation analysis reveals that chaos occurs in the circuit via period-doubling transition and symmetry-restoring crisis scenarios. In addition for a suitable parameters setting and different initial conditions, the circuit exhibits the coexistence of four disconnected periodic and chaotic attractors. This striking feature of the circuit is further characterized by computing the cross sections of the basin of attraction in which we define the set of initial conditions where each attractor can be found. Furthermore, due to the inconveniences of multistability behavior in many nonlinear systems, the control of this phenomenon is discussed by using the linear augmentation scheme. It is proved that by choosing the specific control parameters, the transition from multistable system to monostable system is achieved. Finally, an appropriate electronic circuit capable to emulate the dynamcis of the system is designed and some analog simulations are point out to validate the numerical analysis.

Key words

Chaotic circuit, light-emitting diode, bifurcation analysis, multistability and its control, Pspice based simulations.

1 Introduction

Chaos theory has applications in several fields of studies including, mathematics, physics, chemical reactions, biology, ecology, neural networks, robotics, fuzzy logic, electrical circuits, cryptosystems [Gaspard, 1999; Kyriazis, 1991; Sprott et al., 2005; Aihira et al., 1990; Lankalapalli and Ghosal, 1997; Yau and Shieh, 2008; Matouk and Agiza, 2008; Chien and Liao, 2005] and so on. In the last two decades, considerable efforts have been devoted to the investigation of simple chaotic circuits. The simplicity is in terms of simple mathematical model and minimum number of electronic components used to implement the system. Concerning the latter case, many simple nonlinear chaotic circuits have been reported. Examples include Hartley's oscillator based on a junction field effect transistor and a tapped coil [Pham et al., 2013], two-element memristive time-delay system [Muthuswamy and Chua, 2010], three-element circuit with a nonlinear active memristor [Barboza and Chua, 2008], four-element Chua's circuit, the simple current-tunable chaotic oscillators using floating or virtually grounded diode [Srisuchinwong and Munmuangsaen, 2012] and so on. However, the construction of simple dynamical systems with simple mathematical description is still an open research direction and merit to be explored. In this regard Volos and colleagues [Volos et al., 2017] investigated a simple chaotic circuit with a hyperbolic sine function and exploited in a sound encryption scheme. The dynamics of the system is investigated in terms of phase portraits, Poincaré section, power spectrum, Lyapunov exponents and bifurcation diagram. The experimental verification as well as the application to sound encryption are also included. However, the different bifurcation structures showing different routes to chaos are not investigated in detail. In this contribution, we consider the same model with one novel additional constant parameter in order to make very easy its circuit realization and characterize in detail some dynamical behaviors including bistable phenomenon, symmetry restoring crisis bifurcation and multistability (coexistence of attractors). One of the main motivations of this work is to find the

regions in the parameter space in which the system experiences coexisting attractors in order to control them to a desired state.

The rest of the paper is organized as follows. The mathematical model is presented in Sec. 2. Numerical simulations are investigated in Sec. 3. The dynamics of the model is explored in detail by using some common numerical tools such as time series, phase portrait plots, bifurcation diagrams associated with the largest Lyapunov exponent. The phenomenon of coexisting attractors and its control is examined. In order to verify some dynamical behaviors reported numerically, we present in Sec. 4 some Pspice based analog simulations. The results are compared to those obtained numerical and a good agreement is observed. Some concluding remarks are given in Sec. 5.

2 Mathematical Model

The system investigated in this contribution is the model proposed by Volos and collaborators [Volos et al., 2017] with one novel additional constant parameter namely ρ. The resulting model is given by the following set of three coupled first order nonlinear differential equations:

$$\begin{aligned} \dot{x} &= -y, \\ \dot{y} &= -z, \\ \dot{z} &= -x - \gamma z + \epsilon \sinh(\rho y), \end{aligned} \tag{1}$$

where γ, ϵ, and ρ are are the constant positive parameters. The two later parameters are intrinsic to the light emitting diodes and will be setting constant in section of numerical simulations. It should be mentioned that the new parameter introduced in the original model reported by Volos and colleagues help to facilitate the circuit realization of the mathematical model with a pair of emitting diodes connected in anti-parallel. The great interest devoted to Eq. (1) is justified by its simplicity in the mathematical model (containing only five terms of which one is nonlinear), in the electronic circuit as well as possibility to experience very rich and striking phenomena. Another interesting aspect of Eq. (1) is the configuration (diodes connected in anti-parallel) of light emitting diodes in its electronic circuit which induces the symmetrical features which are necessary for the occurrence of symmetric solutions in the system.

3 Numerical Investigations

3.1 Route to Chaos

In order to explore the rich dynamical behaviors exhibited by Eq. (1), the bifurcation diagram and corresponding Lyapunov spectrum with respect to the parameter γ is examined. Form this study, it is found that the system under investigation can develop very rich and striking bifurcation structures when the considered control parameter is slowly adjusted. As an example,

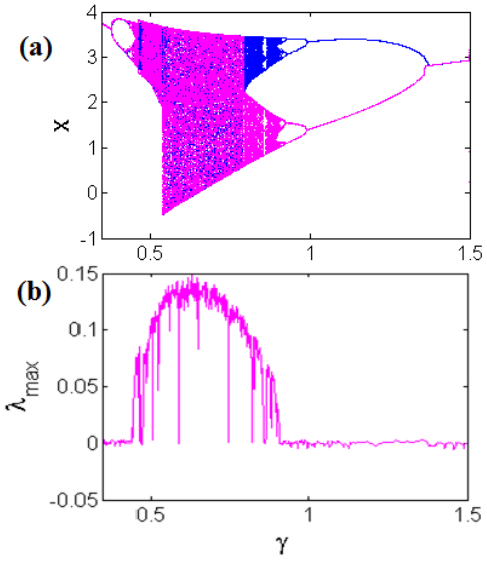

Figure 1. Bifurcation diagram showing the peak of x and corresponding graph of largest Lyapunov exponent with respect to parameter γ for $\epsilon = 2.682 \times 10^{-4}$ and $\rho = 4.0485$.

we show in Fig. 1 the bifurcation diagram showing the peak of state variable x and corresponding graph of largest Lyapunov exponent with respect to the control parameter γ that is increased or (decreased) in tiny steps in the range $0.35 < \gamma < 1.5$ for $\epsilon = 2.682 \times 10^{-4}$ and $\rho = 4.0485$.

It can be observed that the bifurcation diagram well coincides with their corresponding graph of largest Lyapunov exponent. In Fig. 1(a), two sets of data superimposed correspond to the increasing (blue) and decreasing (magenta) value of control parameter, respectively. This method helps to find the regions of hysterical behavior which is responsible to the multiple coexistence of attractors in the system. From Fig. 1, some interesting phenomena such as period-doubling, reverse period-doubling, symmetry restoring crisis, bistability, multistability, limit cycles and chaos are clearly visible. The hysterical phenomenon (responsible of the coexisting attractors), bistability, and symmetry restoring crisis observed in the bifurcation will examined in detail in the following paragraph.

The system in Eq. (1) is symmetric with respect to the origin. This properties induce the bistability phenomenon shown in Fig. 2 in the $(x - y)$ plane for $\epsilon = 2.682 \times 10^{-4}$, $\rho = 4.0485$ and $\gamma = 0.5$.

In Fig. 2, the blue and magenta attractors are obtained, respectively for $x(0), y(0), z(0) = (0, 1, 0)$ and $x(0), y(0), z(0) = (0, -1, 0)$. The phenomena of bistability has been observed in many other nonlinear dynamical systems which possess the symmetrical properties.

For $\epsilon = 2.682 \times 10^{-4}$, $\rho = 4.0485$ and $\gamma = 0.7$, Eq. (1) displays the double-band chaotic attractors follow-

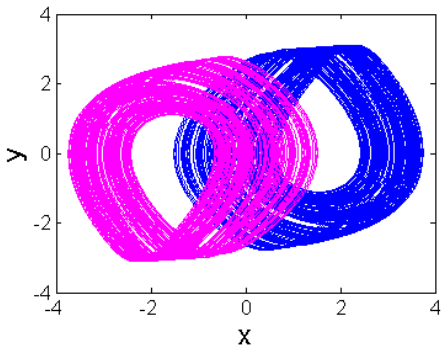

Figure 2. Bistable chaotic attractors in the $(x-y)$ plane obtained for $\epsilon = 2.682 \times 10^{-4}$, $\rho = 4.0485$ and $\gamma = 0.5$. The initial conditions are indicated in the text.

ing a symmetry recovering crisis. The obtained result is depicted in Fig. 3 in the $(x-y)$ plane.

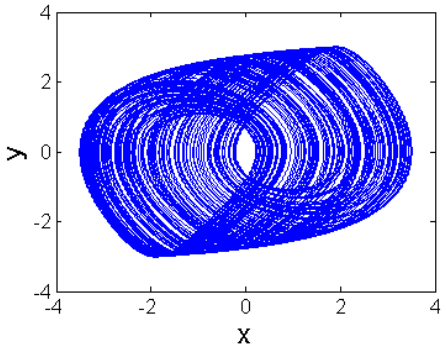

Figure 3. Double-band chaotic attractors in $(x-y)$ plane computed for $\epsilon = 2.682 \times 10^{-4}$, $\rho = 4.0485$ and $\gamma = 0.7$.

In order to illustrate crisis induced intermittency occurring in the system, we provide in Fig. 4 the time traces of coordinate for $\epsilon = 2.682 \times 10^{-4}$, $\rho = 4.0485$ and $\gamma = 0.7$, and different values of γ.

It should be stressed that the crisis route to chaos reported in this work have also been found in various other nonlinear systems [Kengne et al., 2015; Njitacke et al., 2016].

3.2 Hysteresis Dynamics

When we made an enlargement of the bifurcation diagram in the range $0.454 < \gamma < 0.480$, the region in which Eq. (1) experiences hysteresis dynamics is clearly observed as shown in Fig. 5.

In Fig. 5, two sets of data corresponding, respectively, to increasing (blue) and decreasing (magenta) values of the bifurcation control parameter are superimposed. This diagram confirms the existence of the hysterical features in the system described by Eq. (1).

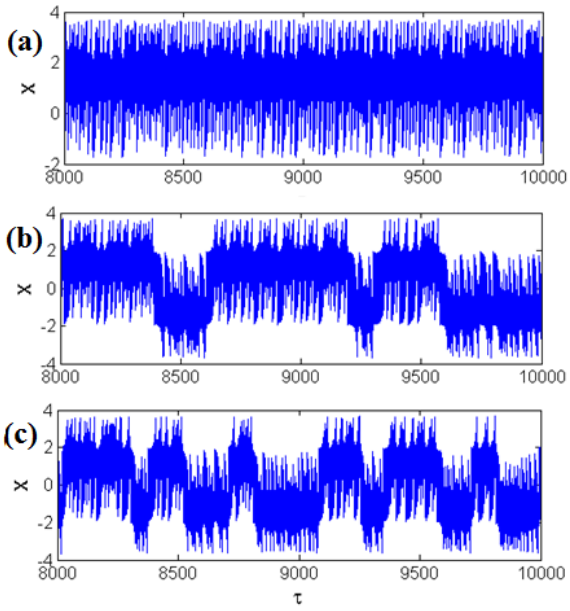

Figure 4. Illustration of symmetry restoring crisis bifurcation for $\epsilon = 2.682 \times 10^{-4}$, $\rho = 4.0485$, (a) $\gamma = 0.5200$, (b) $\gamma = 0.5382$ and (c) $\gamma = 0.5500$. There are two mirror image chaotic attractors one with $x(\tau) < 0$ and another with $x(\tau) > 0$. The two attractors merge to form unique attractor with mirror symmetry.

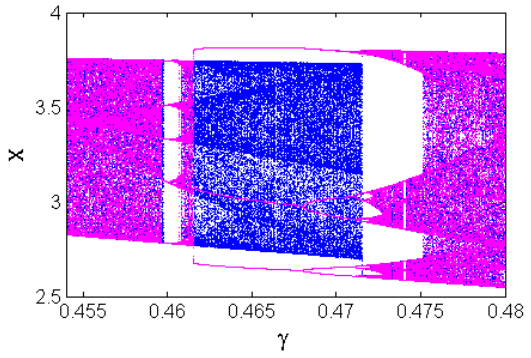

Figure 5. Enlargement of the bifurcation diagram of Fig. 1 in order to make more visible the region in which Eq. (1) exhibits multiple coexisting attractors.

With the same values of parameters setting in Fig. 5, and for $\gamma = 0.462$, the simple jerk circuit with a pair of light emitting diodes displays coexistence of different attractors (i.e., a pair of period-3 limit cycles and a pair of single band chaotic attractors) as shown in Fig. 6. The pair of single-band chaotic attractors are obtained with $x(0), y(0), z(0) = (\pm 0.1, \pm 0.1, \pm 0.1)$ white a pair of period-3 limit cycle are obtained with $x(0), y(0), z(0) = (\pm 1, \pm 1, \pm 1)$. The coexistence of four different solutions is further illustrated by plotting the cross sections of the basin of attraction provided in Fig. 7 for $x(0) = 0$, $y(0) = 0$, and $z(0) = 0$, respectively.

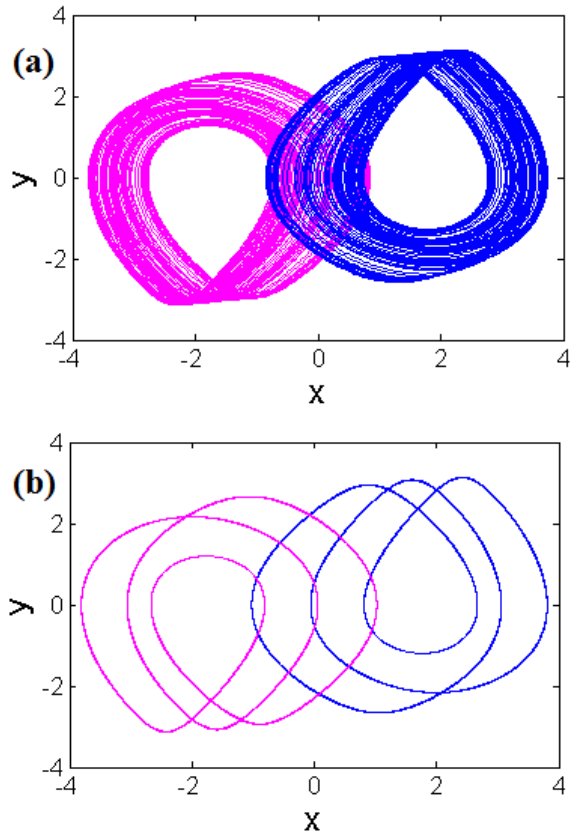

Figure 6. Coexistence of four different attractors for $\epsilon = 2.682\times 10^{-4}$, $\rho = 4.0485$, and $\gamma = 0.462$. The initial conditions are setting as $x(0), y(0), z(0) = (\pm 0.1, \pm 0.1, \pm 0.1)$ and $x(0), y(0), z(0) = (\pm 1, \pm 1, \pm 1)$ for periodic and chaotic solutions, respectively.

One can see from Fig. 7 the different regions of initial conditions in which each attractor can be found. The black regions correspond to initial conditions leading to a pair of chaotic attractors while the yellow ones are associated with the initial conditions leading to a pair of period-3 limit cycles. The coexistence of four different attractors has been reported in other nonlinear systems with complicated model and at least to equilibrium points. The system under investigation in this work is very simpler and possess only one single trivial equilibrium point. This means that the presence of a large number of equilibrium points is not a necessary condition of occurrence of coexisting attractors. It is known that the occurrence of multiple attractors represents an additional form of randomness and system which experience this phenomenon can be used for many applications such as chaos based communication, image encryption and generation of random numbers. However, in many practical situations, this singular phenomenon is not desirable and requires control.

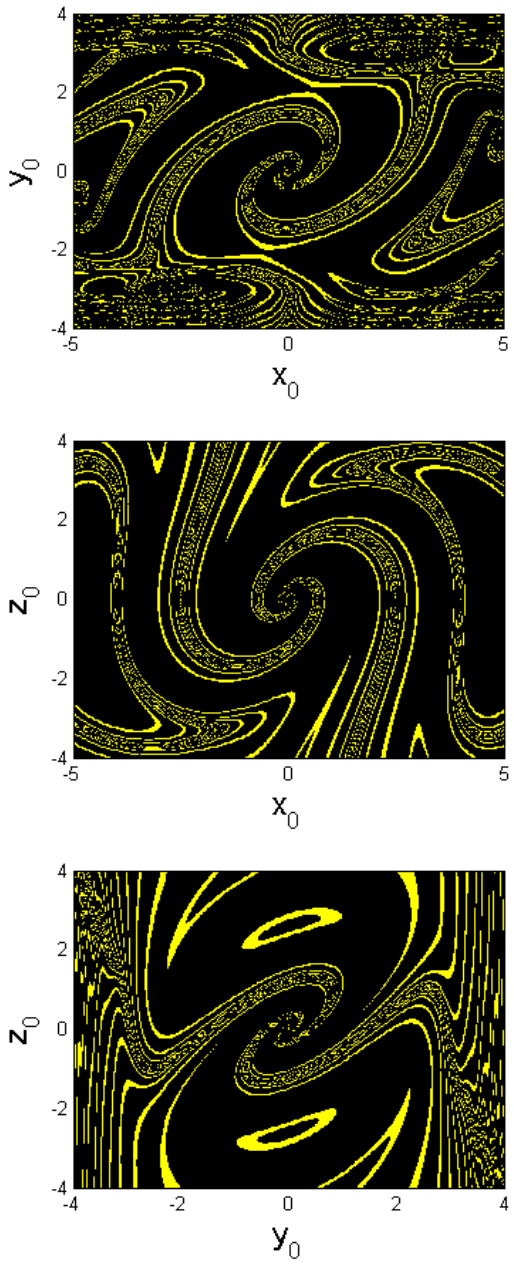

Figure 7. Cross sections of the basin of attraction for $\epsilon = 2.682 \times 10^{-4}$, $\rho = 4.0485$, and $\gamma = 0.462$ for (upper) $z(0) = 0$, (middle) $y(0) = 0$, and (lower) $x(0) = 0$, respectively.

3.3 Control of Multistability

In this section, we discuss the control of mulitstability in Eq. (1) by using the method of linear augmentation [Sharma et al., 2015]. In order to remove multistability behavior, Eq. (1) is coupled with a linear system as follows

$$\begin{aligned} \dot{x} &= -y, \\ \dot{y} &= -z, \\ \dot{z} &= -x - \gamma z + \epsilon \sinh(\rho y) + \alpha w, \\ \dot{w} &= -kw - \alpha(z - \beta), \end{aligned} \tag{2}$$

where α is the coupling strength, β is the control parameter which serves to locate the position of fixed point and k is the decay parameter of the linear system w.

The largest Lyapunov exponent of Eq. (3) in terms of the coupling strength α is presented in Fig. 8.

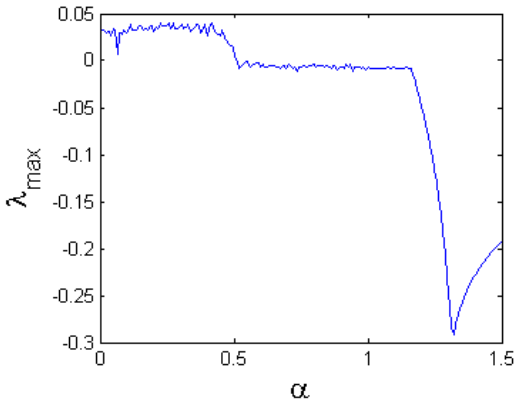

Figure 8. Largest Lyapunov exponent computed with $\epsilon = 2.682 \times 10^{-4}$, $\rho = 4.0485$, $\gamma = 0.462$, $\beta = 0.5$, and $k = 0.7$.

From Fig. 8, one can see that the dynamics of the controlled system in Eq. (3) changes from chaotic to periodic oscillations when the coupling strength is increased. With the same parameters setting in Fig. 6 and for a weak coupling ($\alpha = 0.05$), Eq. (3) displays the coexistence of four different attractors as in Eq. (1) its cross sections of the basin of attraction are similar to those of Fig. 7. For $\alpha = 0.8$, the four coexisting attractors disappear and the system has only a pair of periodic attractors as its basin displayed in Fig. 9.

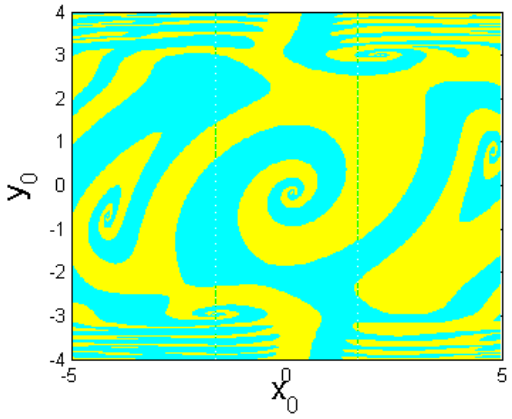

Figure 9. Basin of attraction of a pair of periodic attractors computed $\epsilon = 2.682 \times 10^{-4}$, $\rho = 4.0485$, $\gamma = 0.462$, $\beta = 0.5$, and $k = 0.7$, $\alpha = 0.8$, and $z(0) = w(0) = 0$.

A further increase in the coupling ($\alpha = 1.3$), the linear system kills one periodic attractor and stabilizes the system to a monostable state.

4 Pspice Based Simulations

One of the advantages of analog simulations is the possibility to investigate the dynamical behavior of a circuit by simply varying a single resistor as a control bifurcation parameter. The analog simulations serve to validate the numerical investigations and give some interesting ideas for the real experimental laboratory measurements. The hardware implementation of chaotic models is of great importance for some engineering applications such as chaos based communication, image encryption and random number generation. The purpose of this section is to design an appropriate electronic circuit that can be used to investigate the dynamical behavior of Eq. (1). In this regard, we provide in Fig. 10 the schematic diagram of the electronic circuit capable to emulate the dynamics of Eq. (1).

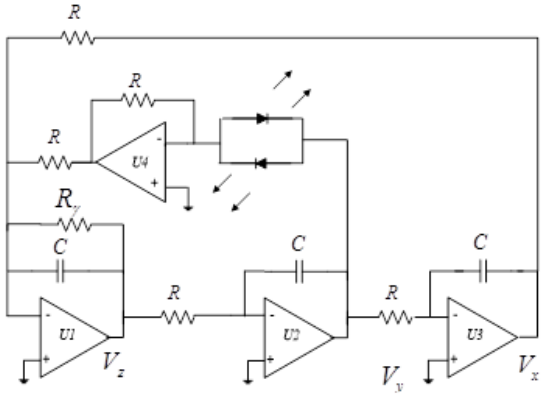

Figure 10. Electronic circuit realization of Eq. (1) with a pair of light emitting diodes.

By using the Kirchhoff's laws into the circuit of Fig. 10, we obtain the mathematical model given by following three differential equations:

$$\begin{aligned} \dot{V_x} &= -\tfrac{1}{RC} V_y, \\ \dot{V_y} &= -\tfrac{1}{RC} V_z, \\ \dot{V_z} &= -\tfrac{1}{RC} V_x - \tfrac{1}{R_\gamma C} V_z + \tfrac{2I_s}{C} \sinh(\tfrac{V_y}{\nu V_T}, \end{aligned} \tag{3}$$

where V_x, V_y, and V_z are the output voltages of the operational amplifiers. The system in Eq. (1) is equivalent to the system in Eq. (**??**) for the following values of the electronic circuit components: $C = 10\ nF$, $R = 10$ kΩ, and R_γ adjustable.

The bistable chaotic attractors depicted in Fig. 11 for $R_\gamma = 11.5$ kΩ.

Similarly, we provided in Fig. 12 the double-band chaotic attractors for $R_\gamma = 14.28$ kΩ.

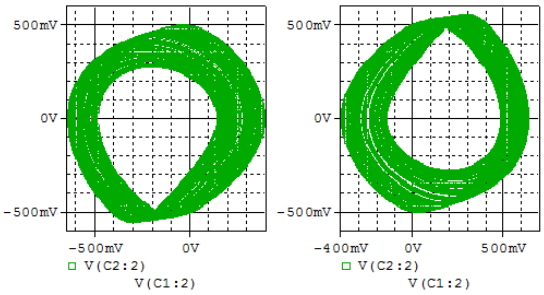

Figure 11. Bistable chaotic attractors obtained for $C = 10$ nF, $R = 10$ kΩ, and $R_\gamma = 11.5$ kΩ. The initial condition setting on the capacitors are setting as $V_x(0), V_y(0), V_z(0) = (\pm 0.1, \pm 0.1, \pm 0.1)$.

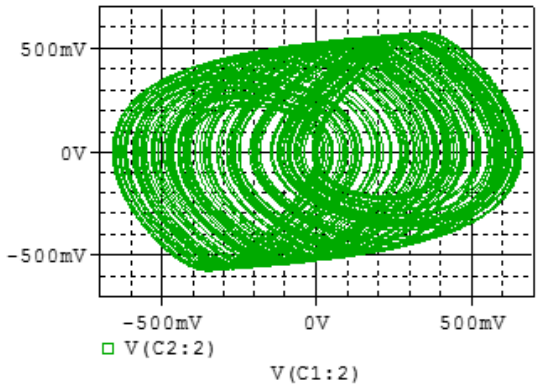

Figure 12. Double-band chaotic attractor obtained for $R_\gamma = 14.28$ kΩ.

One can see that the Pspice based simulations results are in good agreement with those obtained numerically. This serves to justify the ability of the proposed simulator circuit to trace the dynamics of Eq. (1).

5 Conclusion

The dynamics of the simple autonomous like jerk-system with hyperbolic sine function proposed by Volos and coworkers has been detailed in this contribution. Some common tools such as time series plots, phase portraits, bifurcation diagrams and corresponding Lyapunov exponent have been exploited to investigate in detail the dynamical behavior of the system. It is found that the system experiences some interesting phenomena including symmetry restoring crisis, bistability and coexisting attractors. Each phenomenon has been illustrated. In particular for coexisting attractors, the forward and backward bifurcation technique has been used to identify the regions of parameters space showing the occurrence of the hysterical phenomenon responsible of the coexisting attractors exhibited by the circuit. This unusual dynamics has been further investigated by computing the cross sections of the basin of attraction showing the different initial conditions leading to each attractor. The phenomenon of coexisting attractors has been controlled in the system using the linear augmentation technique. The obtained results show that the control method is able to destroy the coexisting attractors and induces the system to a desired trajectory. Furthermore an electronic circuit simulator has been designed and simulated in order to produce some Pspice simulations for the verification of the numerical results.

Acknowledgements

V. K. T. thanks Dr. Sifeu Takougang Kingni from the Department of Mechanical and Electrical Engineering of the University of Maroua, Cameroon for interesting discussions.

References

Gaspard, P. (1999). Microscopic chaos and chemical reactions. *Physica A: Statistical Mechanics and its Applications*, **263**, pp. 315–328.

Kyriazis, M. (1991). Applications of chaos theory to the molecular biology of aging. *Experimental Gerontology*, **26**, pp. 569–572.

Sprott, J. C., Vano, J. A., Wildenberg, J. C., Anderson, M. B., and Noel, J. K. (2005). Coexistence and chaos in complex ecologies. *Physics Letters A*, **335**, pp. 207–212.

Aihira, K., Takabe, T., and Toyoda, M. (1990). Chaotic neural networks. *Physics Letters A*, **144**, pp. 333–340.

Lankalapalli, S. and Ghosal, A. (1997). Chaos in robot control equations. *Int. J. Bifurc. Chaos*, **7**, pp. 707–720.

Yau, H. T. and Shieh, C. S. (2008). Chaos synchronization using fuzzy logic controller. *Nonlinear Analysis: Real World Applications*, **9**, pp. 1800–1810.

Matouk, A. E. and Agiza, H. N. (2008). Bifurcations, chaos and synchronization in ADVP circuit with parallel resistor. *Journal of Mathematical Analysis and Applications*, **341**, pp. 259–269.

Chien, T. I. and Liao, T. L. (2005). Design of secure digital communication systems using chaotic modulation, cryptography and chaotic synchronization. *Chaos, Solitons and Fractals*, **24**, pp. 241–245.

Pham, V. T., Buscarino, A., Fortuna, L., and Frasca, M. (2013). Simple memristive time-delay chaotic systems. *Int. J. Bifurc. Chaos*, **23**, art no. 1350073.

Muthuswamy, B. and Chua, L. O. (2010) Simplest chaotic circuit. *Int. J. Bifurc. Chaos*, **20**, pp. 1567–1580.

Barboza, R. and Chua, L .O. (2008). The four-element Chuas circuit. *Int. J. Bifurc. Chaos*, **18**, pp. 943–955.

Srisuchinwong, B. and Munmuangsaen, B. (2012) Four current-tunable chaotic oscillators in set of two diode-reversible pairs. *Electron. Lett.*, **48**, pp. 1051–1053.

Volos, C., Akgul, A., Pham, V. T., Stouboulos, I., and Kyprianidis. I. (2017). A simple chaotic circuit with

a hyperbolic sine function and its use in a sound encryption scheme. *Nonlinear Dyn.*, **89**, pp 1047–1061.

Kengne, J., Njitacke, Z. T., Nguomkam Negou, A., Fouodji Tsotsop, M., and Fotsin, H. B (2015). Coexistence of multiple attractors a nd crisis route to chaos in a novel chaotic jerk circuit. *Int. J. Bifurc. Chaos*, **25**, art. no. 1550052.

Njitacke Z. T., kengne J., Fotsin H.B, Nguomkam Negou A, and Tchiotsop D (2016). Coexistence of multiple attractors a nd crisis route to chaos in a novel memristive diode bidge-based Jerk circuit. *Chaos, Solitons and Fractals*, **91**, pp. 180–197.

Sharma, P. R., Shrimali, M. D., Prasad, A., Kuznetsov, N. V., and Leonov, G. A. (2015). Control of multistability in hidden attractors. *Eur. Phys. J. Special Topics*, **224**, pp. 1485–1491.